ACS APPLIED MATERIALS & INTERFACES

Research Article

www.acsami.org

Investigation of Regeneration Kinetics in Quantum-Dots-Sensitized Solar Cells with Scanning Electrochemical Microscopy

Bingyan Zhang, Huailiang Yuan, Xiaofan Zhang, Dekang Huang, Shaohui Li, Mingkui Wang, and Yan Shen*

Wuhan National Laboratory for Optoelectronics, School of Optoelectronic Science and Engineering, Huazhong University of Science and Technology, Wuhan 430074, P. R. China

Supporting Information

ABSTRACT: A fast quantum dots (QDs) regeneration process is necessary for highly efficient QDs-sensitized solar cells. Herein, CdSe and CdS QDs regeneration rates (k_{QD}') in three redox electrolytes, which are triiodide and iodide ions (I_3^-/I^-), $Co(bpy)_3(PF_6)_2$ and $Co(bpy)_3(PF_6)_3$ (Co^{3+}/Co^{2+}), and 1-methy-1-H-tetrazole-5-thiolate and its dimer (T_2/T^-), have been first investigated with scanning electrochemical microscopy (SECM). The results reveal that the kinetics of QDs regeneration depends on the nature of the QDs and the redox shuttles presented in QDSSCs. For QDs of CdSe and CdS, the regeneration rate (k_{QD}') in the case of a T_2/T^--based electrolyte is about two times larger than that of Co^{3+}/Co^{2+} and I_3^-/I^-. Additionally, the k_{QD}' for CdSe is about two times larger than that of CdS in the same redox shuttle electrolyte, which could be due to a large driving force for the reaction between the exited state quantum dots (QD^+) and redox electrolytes.

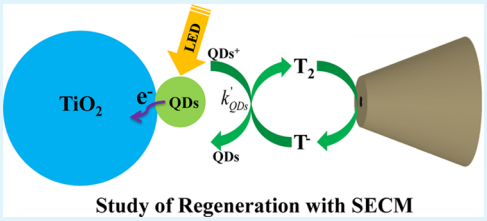

KEYWORDS: *regeneration kinetics, scanning electrochemical microscopy, quantum dots, solar cell, interfacial charge transfer*

1. INTRODUCTION

Solar energy has been considered as an ideal renewable energy to meet human beings' demands. It requires new initiatives to convert incident photons to electricity with high efficiency. Nanostructured semiconductors and molecular assemblies have been widely investigated for this purpose.[1−4] Particularly, dye sensitization of mesoscopic TiO_2 has attracted increasing attention as an alternative to the conventional silicon-based photovoltaic.[5,6] Recently, development of sensitizers and redox shuttles used in DSSC devices has led to remarkable solar photovoltaic power conversion efficiencies (PCE) in the range of 11−13%.[7,8] Even higher PCE, as high as 15%, has been achieved with perovskite-sensitized mesoporous solar cells.[9,10] Over the recent years, inorganic semiconductor quantum dots (QDs) have attracted great interest due to their unique optoelectronic properties derived from the quantum confinement effect. Their size quantization property allows tuning the visible response and varying the band offsets for modulation of the vectorial charge transfer and photoresponse as well as PCE of solar cells.[11−13]Narrow band gap QDs semiconductors such as CdS,[14,15] PbS/CdS,[16] Sb_2S_3/CuSCN,[17] CdSe,[5,12,18,19] CdSe/CdTe,[20] and $CuInS_2$[21] are suitable for sensitized solar cells (coded as QDSSCs) because they can transfer electrons to large band gap semiconductors such as TiO_2 or SnO_2 under visible light excitation. Recently, the PCE of QDSSCs has been improved to exceed 4% under AM 1.5G one sun irradiation with the most widely used QDs materials including CdS, CdSe,[22−25] and $CuInSe_xS_{2-x}$.[26,27] Pan et al. reported that the PCE of QDSSCs based on $CuInS_2$ could be increased to a record of 7.04%.[28]

However, the development of QDSSCs has been limited due to the lack of efficient electrolytes. The most common example of redox electrolytes in QDSSCs is polysulfide (S^{2-}/S_n^{2-}),[11,29−31] where it shows superior properties in conjunction with sulfide-containing QDs. It has been widely accepted that a big challenge still remains for the complicate redox reaction of polysulfide electrolyte in terms of suitable counter electrodes.[32] Up to now, most reported QDSSC devices based on polysulfide (S^{2-}/S_n^{2-}) electrolyte presented weak abilities of the polysulfide redox couple in the hole-recovery, high charge-recombination rate at the QDs-sensitized electrode/electrolyte interface, and improper utilization of the counter electrode, which would lead to a low fill factor (FF) and open circuit photovoltage (V_{oc}), and eventually restricted device efficiency.[33] A large amount of efforts have been made to search for new electrolytes, such as Co^{3+}/Co^{2+},[34,35] Fe^{3+}/Fe^{2+}, $Fe(CN)_6^{3-}/Fe(CN)_6^{4-}$,[31] 2-mercapto-5-methyl-1,3,4-thiadiazole/disulfide dimer (McMT/BMT),[33] and T_2/T^-.[36] For example, cobalt complex (Co^{3+}/Co^{2+}) has been used as redox couple to perform stable and reproducible $I-V$ characterization on PbS-, CdS-, and CdSe-sensitized cells with an overall conversion efficiency of over 1.7% at 0.1 sun and 1% at full sun intensity, although this electrolyte suffers from slow ion conductivity which allows efficient operation only under low light intensities.[34,35]

In QDSSC devices, the excited state energy level of QDs sensitizers should be more negative than that of the conduction

Received: August 19, 2014
Accepted: November 14, 2014
Published: November 14, 2014

band edge (vs NHE) of the semiconductor for an efficient electron injection process from sensitizers to semiconductors, and similarly, the oxidized state energy level of QD sensitizers must be more positive than that of redox shuttle electrolytes (vs NHE) for efficient regeneration. Previous studies have analyzed the effect of electrolytes on dye regeneration, being highly related to the photovoltaic performance of DSSC devices.[37−40] In the past years, the detailed investigation on the mechanism for dye-generation in DSSCs has been performed with spectroscopy and spectroelectrochemistry techniques or photoelectrochemistry characterization of an individual electrode or a completed cell.[37,41−43] The dye regeneration reaction can also be studied by nanosecond transient absorption spectroscopy (TAS), which provides valuable information for understanding sensitized solar cells.[34,40,44,45] Recently, Kongkanand et al. has used the nanosecond laser TAS to measure the rate of quantum dots regeneration that the hole was scavenged from CdSe by S^{2-}.[29] Scanning electrochemical microscopy (SECM) is an effective technique to determine interfacial charge transfer kinetics, including solid/liquid interface and liquid/liquid interface.[46,47] The application of SECM to investigate charge transfer kinetics between I^- and photo-oxidized dyes molecule ($Eosin\ Y^+$) adsorbed on ZnO was first reported by Wittstock et al., demonstrating the viability of this method for understanding of DSSCs.[48] Compared to the nanosecond laser TAS characterization, SECM is suitable to monitor the fast interfacial electron or hole transfer process in devices under working condition.[48−50]

In this study, the QDs (CdSe, CdS) regeneration rate (k_{QD}') in three redox electrolytes with acetonitrile as solvent, which include iodide ions (I^-), $[Co(bpy)_3]^{2+}$ and 1-methy-1-H-tetrazole-5-thiolate (T^-), was investigated with SECM. Figure 1

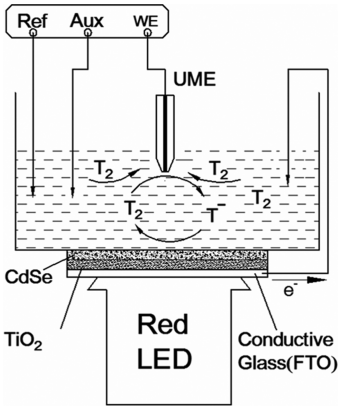

Figure 1. Basic arrangement for probing the heterogeneous reaction at an n-type quantum-dot-sensitized semiconductor (TiO_2) surface in the feedback mode of SECM under short-circuit conditions.

presents the basic arrangements for the SECM investigation of heterogeneous reaction at the QDs-sensitized semiconductor surface with feedback mode under short-circuit condition. We provided a thorough experimental verification of feedback mode to compare the kinetics for quantum dots regeneration by using above redox shuttles. A theoretical model was applied to interpret the current response at the tip under short-circuit condition, thus important information on factors that govern the dynamics of QDs regeneration was obtained.

2. EXPERIMENTAL SECTION

Tetrabutyl ammonium perchlorate (TBAP) was used as supporting electrolyte. SECM experiments were performed on a CHI 920C electrochemical workstation (CH Instruments, Shanghai). A home-made Teflon cell (with volume of 2 mL) was used to hold a Pt wire counter electrode and an Ag/Ag^+ reference electrode. The photoanodes $FTO/TiO_2/CdSe$, $FTO/TiO_2/CdS$ sample films were attached to the cell bottom and sealed with an O-ring as work electrode. In the SECM measurement, the quantum-dots-sensitized transparent semiconductor nanocrystal films (TiO_2 with a thickness of about 10.0 μm) were used as the working electrode. An extra Pt wire was connected to an FTO substrate with the electrolyte in order to operate the photoelectrochemical cell in a short-circuit setup (Figure 1). A 25 μm diameter Pt wire (Goodfellow, Cambridge, UK) was sealed into a 5 cm glass capillary prepared by a Vertical pull pin instrument (PC-10, Japan). The ultramicroelectrode (UME) was polished by a grinding instrument (EG-400, Japan) and micropolishing cloth with 1.0, 0.3, and 0.05 μm alumina powder. Then the UME was sharpened conically to a RG of 10, where RG is the ratio between the diameters of the glass sheath and the Pt disk. All experiments were carried out at room temperature. The irradiation was focused onto the backside of the photoanode from a light emitting diode (red, Lumileds Lightin, USA).

The potential of the UME (E_T) was selected well in the region of the steady diffusion current after recording the cyclic voltammograms (CV) of redox shuttles at 0.1 mM (Figure S1). The feedback mode of SECM was used in this work. The basic arrangements for probing the heterogeneous reaction at quantum-dots-sensitized TiO_2 in the feedback mode of SECM under short-circuit conditions are shown in Figure 1. And the detailed process for the quantum dots photoanode fabrication and characterzation has been set in the Supporting Information.

Here it is worthwhile to point out that only iodine-based electrolyte is corrosive toward QDs among the three redox shuttles. So QDs in I_3^-/I^- electrolyte show poor stability, and the power conversion efficiency of the device based on I_3^-/I^- decreases quickly in a short period of time. The power conversion efficiency of the devices based on Co^{3+}/Co^{2+} and T_2/T^- would remain unchanged for a long time because the QDs in these two electrolytes can show a better stability.

3. RESULTS AND DISCUSSION

In the present work, three redox shuttles, including triiodide and iodide (coded as I_3^-/I^-), $Co(bpy)_3(PF_6)_2$ and $Co(bpy)_3(PF_6)_3$ (coded as Co^{3+}/Co^{2+}), and 1-methy-1-H-tetrazole-5-thiolate and its dimer (coded as T^-/T_2),[51] are used. The molecular structures of the redox shuttles are illustrated in Figure 2a. The UV−visible absorption spectra of CdSe and CdS QDs-sensitized TiO_2 films are presented in Figure 2b. An absorption in the range from 400 to 700 nm was observed for CdSe-sensitized TiO_2 films, which was wider than that of CdS-sensitized TiO_2 sample (being in the range from 400 to 600 nm). Moreover, it was observed that the intensity of the spectral absorption of $CdSe/TiO_2$ was much stronger than that of CdS/TiO_2 with the same film thickness. The UV−visible light absorption of the CdSe and CdS QDs-sensitized films would lead to the difference in photovoltaic performance of QDSSC devices.[30] Herein, SECM was employed to scrutinize the effect of different redox couples on the quantum dots regeneration rate. The aim is to exploit the influence of redox couples and sensitizers on the QDs regeneration kinetics. The SECM measurements with feedback mode were performed under short-circuit conditions to investigate the reduction of the oxidized QDs cation at the nanocrystalline/electrolyte heterojunction. The measurement is based on monitoring the feedback current, which is related to the very small change in the concentration of the redox shuttle under the active area of

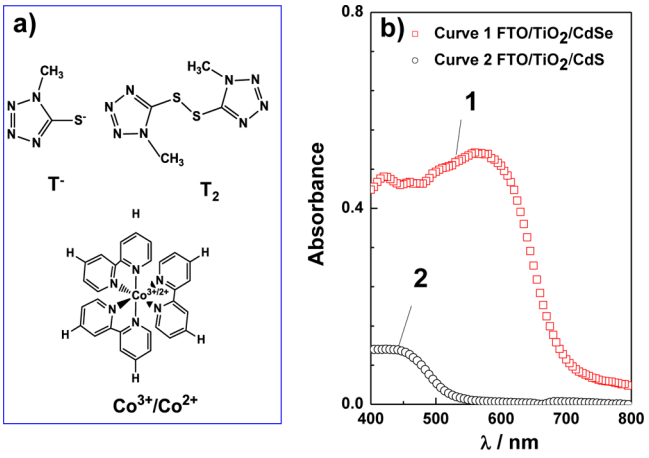

Figure 2. (a) Molecular structure of the redox shuttles used in this study: 1-methy-1-H-tetrazole-5-thiolate (T^-), its dimer (T_2), and Co^{3+}/Co^{2+}. (b) UV−visible absorption spectra of CdSe and CdS quantum-dots-sensitized TiO_2 films.

an ultramicroelectrode (UME) probe caused by the regeneration of the QDs sensitizer. According to the inverse relationship between the effective heterogeneous rate constant k_{eff} and the concentration of redox shuttles, a lower concentration of redox shuttles would induce higher k_{eff} values, which is easier for SECM measurements.[S2] The QDs regeneration kinetics was investigated on the photoanode (i.e., TiO_2/CdSe and TiO_2/CdS) in the presence of the oxidized species of the redox couple. It is worthwhile to state that the concentrations of these three redox couples used in SECM tests are very low (0.1−1 mM), which are about 3 orders of magnitude lower than that of a complete QDSSC device. There are two reasons for this arrangement, one reason is the SECM measurements with feedback mode should be performed at low concentration of redox electrolyte; the other one is that I_3^-/I^- electrolyte with low concentration could reduce the corrosion toward QDs. Figure 3 presents a typical

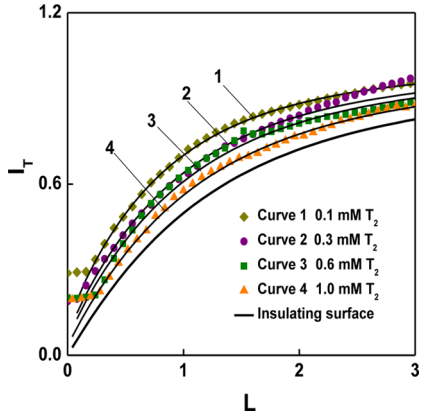

Figure 3. Normalized SECM feedback approach curves for the approach of a Pt ultramicroelectrode toward a FTO/TiO_2/CdSe film with various concentrations of redox mediators (T_2), under illumination by a red light LED at a constant intensity J_{hv} of 14.7 × 10^{-9} mol cm^{-2} s^{-1}, scan rate = 1 μm s^{-1}, $E(T,T_2)$ = −1.2 V (vs Ag/Ag^+), and r_T = 12.5 μm. Solid lines are calculated curves for the approach of a UME with RG = 10 toward an inert insulating surface (line at the bottom), and toward samples with first-order kinetics of mediator recycling using normalized rate constant κ: (1) 0.065; (2) 0.0230; (3) 0.018; (4) 0.014.

approach curve (tip current−distance relationships) for the case of TiO_2/CdSe in T_2 electrolyte, with various concentrations under illumination by a red light LED at a constant intensity serving as an example. Other approach curves and their evaluation for various QDs redox couples are shown in Figures S2−S6 (section SI-3 in the Supporting Information). The normalized tip current I_T ($=i_T/i_{T,\infty}$) is related to the tip current (i_T) and the steady-state current ($i_{T,\infty}$) at semi-infinite height. L ($=d/r_T$) is the normalized tip height, where d is the distance between the tip and substrate electrode and with r_T being the radius of the active area of the SECM tip. As shown in Figure 3, the interfacial charge transfer dominates the current curves when the tip approaches the sample surface. The important kinetic parameter (i.e., the normalized apparent heterogeneous electron transfer rate constant κ) can be obtained by fitting the approach curves with eqs S1−S5 in the Supporting Information. Compared to the I_T^{ins} (i.e., the current recorded with an inert insulating surface, the solid line at the bottom in Figure 3), the normalized tip current I_T (i.e., the current recorded above an illuminated quantum-dots-sensitized film, dot lines with different shapes) showed much higher values, indicating a positive feedback in this case. Based on the normalized apparent heterogeneous electron transfer rate constant κ, the effective heterogeneous rate constant k_{eff} (in cm s^{-1}) can be evaluated with the equation $k_{eff} = \kappa D/r_T$, where D is the diffusion coefficient for the redox shuttle in acetonitrile electrolyte solution and the diffusion coefficients D of redox shuttles are shown in Table 1.

Table 1. Diffusion Coefficients (D) of Redox Active Species in Various Electrolytes[6]

redox shuttles	diffusion coefficient [10^{-5} cm^2 s^{-1}]
T_2	1.76
Co^{3+}	1.17
I_3^-	1.37

We first evaluated the influence of redox shuttles on the regeneration for TiO_2 sensitized with CdSe and CdS. Figure 4 presents the k_{eff} for the CdSe and CdS QDs-sensitized TiO_2 films in the solutions containing T_2, Co^{3+}, and I_3^- at a constant illumination intensity supported by a red LED. The k_{eff} decreases with increasing concentration of T_2, Co^{3+}, or I_3^-. It was observed that the k_{eff} for T_2 was larger than for Co^{3+} or I_3^- in the case of CdSe or CdS, among which the TiO_2/CdSe/electrolyte interface showed a faster apparent regeneration process. This result agrees with the report that the T_2/T^- redox shuttle can be used as an effective electrolyte in QDSSCs.[33,36]

Therefore, the constants k_{QD}' for the regeneration of the photoexcited QDs by the redox shuttle QDSSCs at a given incident light intensity can be obtained with eq 1.[53]

$$k'_{QD} = \frac{2k_{eff}\phi_{hv}J_{hv}}{6k_{eff}[C] - 3l[S]\phi_{hv}J_{hv}} \quad (1)$$

where [C] is the concentration of redox shuttle in electrolyte (mol cm^{-3}), l is the film thickness (cm), [S] is the volumetric concentration of the quantum dots on the film (mol cm^{-3}), J_{hv} is the incident photon flux (mol cm^{-2} s^{-1}), and ϕ_{hv} is the excitation cross-section of the sensitizer molecules (cm^2 mol^{-1}), respectively.

The heterogeneous rate constants (k_{QD}') for the regeneration kinetics of the photoexcited quantum dots (CdSe and

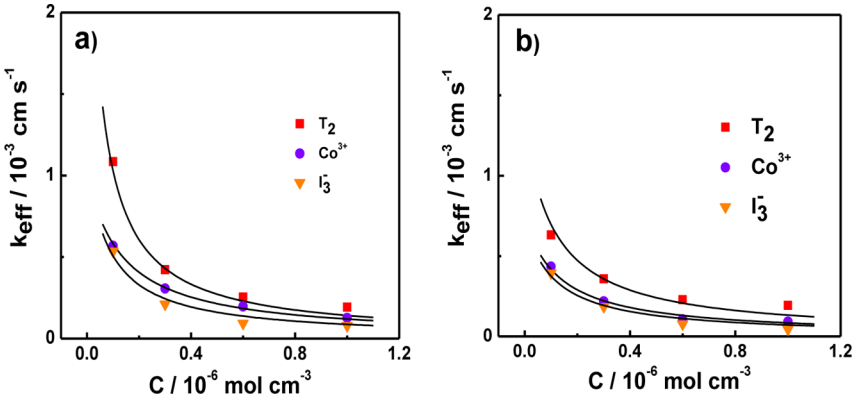

Figure 4. Plot of k_{eff} vs $[T_2]$, $[Co^{3+}]$, and $[I_3^-]$ with different concentrations for (a) CdSe and (b) CdS quantum-dots-sensitized TiO_2 photoelectrochemical electrodes in acetonitrile. The full data sets are presented in Supporting Information section SI-4. The solid lines represent different fits of parameters to the data by using eq 1. The fitting parameters are given in Table 2.

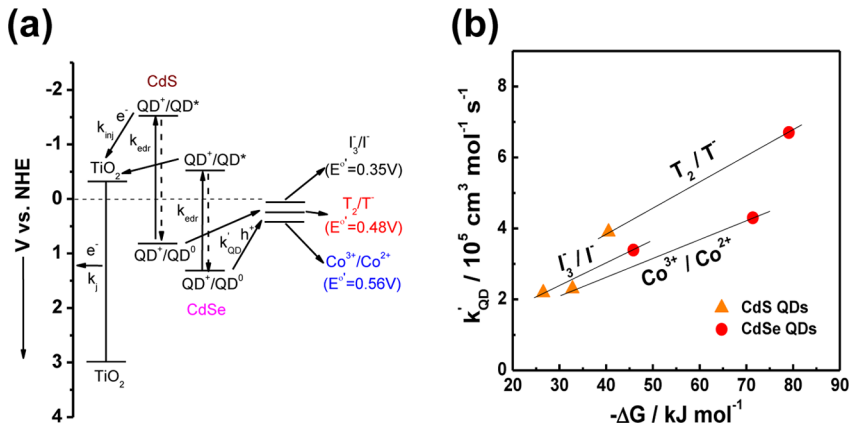

Figure 5. (a) Energy band structure of TiO_2/CdSe, TiO_2/CdS, and the redox potential ($E°'$) of the redox shuttles, T_2/T^-, Co^{3+}/Co^{2+}, and I_3^-/I^-. (b) Plot of k_{QD}' vs $-\Delta G$ with different redox shuttles for CdSe and CdS QDs.

CdS) reduced by the T^-, I^-, or Co^{2+}, the excitation cross-sections of the molecular quantum dots (ϕ_{hv}), and the volumetric concentrations of the quantum dots [S] were obtained by fitting the k_{eff} vs [C] curve (Figure 4) based on eq 1. It was observed that the excitation cross-section (ϕ_{hv}) of CdSe was a little larger than that of CdS quantum dots under the same illumination conditions, and the redox shuttle has nearly no effect on the excitation cross-section. For a given redox shuttle concentration [C] and light intensity (J_{hv}), significantly larger k_{QD}' values for CdSe compared to CdS quantum dots were obtained with the three redox shuttles of T_2/T^-, Co^{3+}/Co^{2+}, and I_3^-/I^-. This could be attributed to the oxidized state energy level of CdSe QDs sensitizer (QD^+) being more positive than the redox potential of the electrolytes, which would lead to a larger driving force ($-\Delta G$) of quantum dots regeneration (Figure 5a). The driving force for QDs regeneration, $-\Delta G$, is commonly estimated according to eq 2:[40]

$$-\Delta G = \nu e \Delta E = \nu e[E_{1/2}(QD^+/QD^0) - E_{1/2}(\text{electrolyte})] \quad (2)$$

where $E_{1/2}(QD^+/QD^0)$ and $E_{1/2}$(electrolyte) are the redox potentials of the QDs and the redox shuttles, respectively. ν is the number of electrons transferred, and e is the elemental charge of the electron. The relationship between rate constants (k_{QD}') and drive force ($-\Delta G$) is presented in Figure 5b, showing an exponential increase of rate constant with the drive force. It was accepted that the regeneration kinetics can be affected by the driving force for the reaction between the excited sensitizers and redox electrolyte. The QDs regeneration rate value of k_{QD}' with the mediator of T_2 was about two times larger than Co^{3+} and I_3^- for the case of CdSe- and CdS-sensitized TiO_2/electrolytes interfaces. The k_{QD}' of T_2 electrolyte was evaluated to be 6.7×10^5 and 3.9×10^5 mol^{-1} cm^3 s^{-1} for CdSe and CdS, respectively (Table 2). The

Table 2. Fitting Results for Experimental k_{eff} vs [C]*[a]

	ϕ_{hv} [cm^2 mol^{-1}]		k_{QD}' [mol^{-1} cm^3 s^{-1}]	
redox shuttles	CdSe	CdS	CdSe	CdS
T_2/T^-	6.01×10^6	5.1×10^6	6.70×10^5	3.90×10^5
Co^{3+}/Co^{2+}	6.00×10^6	5.0×10^6	4.30×10^5	2.30×10^5
I_3^-/I^-	6.01×10^6	5.0×10^6	3.39×10^5	2.19×10^5

[a]Figure 4, Table S1; $l = 1.0 \times 10^{-3}$ cm, [CdSe] = 3.36×10^{-6} mol cm^{-3}, [CdS] = 2.16×10^{-6} mol cm^{-3}.

T_2/T^- redox couple has a chemical composition similar to the polysulfide (S^{2-}/S_n^{2-}) electrolyte toward a redox reaction, exhibiting stable properties during the SECM measurement.[6] As shown in Figure 5a, for example, the redox potential of T_2/T^- is more negative than that of Co^{3+}/Co^{2+}, which leads to a larger driving force for the holes transferring from the valence band to redox electrolytes in the process of QD regeneration. Here, we should point out that a lower k_{QD}' for I_3^-/I^-

electrolyte is observed though the drive force ($-\Delta G$) is the largest in this case (Figure 5b). This could be due to the fact that the regeneration reaction with I_3^-/I^- has to go through two steps that include I_3^-/I^- and I_2^-/I^-, which leads to a large loss in potential energy.[54]

Figure S7 and Table S2 present the photovoltaic performance of the cells using CdS and CdSe in combination with various redox shuttles. It was observed that the devices using CdS QDs with these three redox shuttles showed a lower short-circuit photocurrent density compared with the devices based on CdSe QDs. This result might be attributed to the different light absorbance performances of these two QDs. The QDs regeneration rate value k_{QD}' also may play an important role in the photocurrent enhancement. CdSe QDs show a higher k_{QD}' than that of CdS among the three redox shuttles (Table 2). A higher k_{QD}' of CdSe QDs would be helpful for reduction of charge recombination, thus improving charge collection and eventually the photocurrent (Table S2).

4. CONCLUSIONS

The regeneration kinetics (k_{QD}') at the QDs-sensitized semiconductors/electrolytes interface was first investigated by SECM approach curves based on the feedback mode. A rate constant of k_{QD}' with different redox shuttles concentrations was determined for the regeneration process of quantum dots. Approach curves in SECM measurements showed that the kinetics of QDs regeneration depends on the nature of QDs and redox shuttles presented in QDSSCs. For QDs of CdSe and CdS, the regeneration rate (k_{QD}') in the case of T_2/T^--based electrolyte is about two times larger than that of Co^{3+}/Co^{2+} and I_3^-/I^-. The sufficient driving force for quantum dots regeneration obtained by T_2/T^- is also an important reason for the quick regeneration kinetics (k_{QD}') and an important parameter for the design of efficient QDSSCs. This work would offer some new complementing aspects to establish the methods for QDSSCs characterization by testing of different redox mediator electrolytes and quantum dots with a single quantum-dots-sensitized electrode.

■ ASSOCIATED CONTENT

Supporting Information

Quantum dots photoanode fabrication, device characterization, SECM measurements, approach curves, and calculated data from SECM measurements. This material is available free of charge via the Internet at http://pubs.acs.org.

■ AUTHOR INFORMATION

Corresponding Author

*E-mail: ciac_sheny@mail.hust.edu.cn.

Notes

The authors declare no competing financial interest.

■ ACKNOWLEDGMENTS

We gratefully acknowledge the 973 Program of China (2014CB643506, 2013CB922104, and 2011CBA00703), NSFC (21103578, 21161160445, and 201173091), and the Fundamental Research Funds for the Central Universities (HUST: CXY12Q022 and 2013YQ051). The authors acknowledge the Analytical and Testing Center of Huazhong University of Science and Technology for support.

■ REFERENCES

(1) Nozik, A. J.; Beard, M. C.; Luther, J. M.; Law, M.; Ellingson, R. J.; Johnson, J. C. Semiconductor Quantum Dots and Quantum Dot Arrays and Applications of Multiple Exciton Generation to Third-Generation Photovoltaic Solar Cells. *Chem. Rev.* **2010**, *110*, 6873−6890.

(2) Ameri, T.; Li, N.; Brabec, C. J. Highly Efficient Organic Tandem Solar Cells: A Follow up Review. *Energy Environ. Sci.* **2013**, *6*, 2390−2413.

(3) Bai, Y.; Mora-Sero, I.; De Angelis, F.; Bisquert, J.; Wang, P. Titanium Dioxide Nanomaterials for Photovoltaic Applications. *Chem. Rev.* **2014**, DOI: 10.1021/cr400606n.

(4) Kumar, S. G.; Rao, K. S. R. K. Physics and Chemistry of CdTe/CdS Thin Film Heterojunction Photovoltaic Devices: Fundamental and Critical aspects. *Energy Environ. Sci.* **2014**, *7*, 45−102.

(5) Robel, I.; Subramanian, V.; Kuno, M.; Kamat, P. V. Quantum Dot Solar Cells. Harvesting Light Energy with CdSe Nanocrystals Molecularly Linked to Mesoscopic TiO_2 Films. *J. Am. Chem. Soc.* **2006**, *128*, 2385−2393.

(6) Zhang, B.; Xu, X.; Zhang, X.; Huang, D.; Li, S.; Zhang, Y.; Zhan, F.; Deng, M.; He, Y.; Chen, W.; Shen, Y.; Wang, M. Investigation of Dye Regeneration Kinetics in Sensitized Solar Cells by Scanning Electrochemical Microscopy. *ChemPhysChem* **2014**, *15*, 1182−1189.

(7) Mathew, S.; Yella, A.; Gao, P.; Baker, R. H.; Curchod, B. F. E.; Astani, N. A.; Tavernelli, I.; Rothlisberger, U.; Nazeeruddin, M. K.; Grätzel, M. Dye-sensitized Solar Cells with 13% Efficiency Achieved Through the Molecular Engineering of Porphyrin Sensitizers. *Nat. Chem.* **2014**, *6*, 242−247.

(8) Yella, A.; Lee, H. W.; Tsao, H. N.; Yi, C.; Chandiran, A. K.; Nazeeruddin, M. K.; Diau, E. W.; Yeh, C. Y.; Zakeeruddin, S. M.; Grätzel, M. Porphyrin-Sensitized Solar Cells with Cobalt (II/III)-Based Redox Electrolyte Exceed 12% Efficiency. *Science* **2011**, *334*, 629−634.

(9) Burschka, J.; Pellet, N.; Moon, S. J.; Humphry-Baker, R.; Gao, P.; Nazeeruddin, M. K.; Grätzel, M. Sequential Deposition as A Route to High-Performance Perovskite-Sensitized Solar Cells. *Nature* **2013**, *499*, 316−319.

(10) Zhou, H.; Chen, Q.; Li, G.; Luo, S.; Song, T. B.; Duan, H. S.; Hong, Z.; You, J.; Liu, Y.; Yang, Y. Photovoltaics. Interface Engineering of Highly Efficient Perovskite Solar Cells. *Science* **2014**, *345*, 542−546.

(11) Kamat, P. V. Quantum Dot Solar Cells. Semiconductor Nanocrystals as Light Harvesters. *J. Phys. Chem. C* **2008**, *112*, 18737−18753.

(12) Kongkanand, A.; Tvrdy, K.; Takechi, K.; Kuno, M.; Kamat, P. V. Quantum Dot Solar Cells. Tuning Photoresponse Through Size and Shape Control of CdSe-TiO_2 Architecture. *J. Am. Chem. Soc.* **2008**, *130*, 4007−4015.

(13) Ruhle, S.; Shalom, M.; Zaban, A. Quantum-Dot-Sensitized Solar Cells. *ChemPhysChem* **2010**, *11*, 2290−2304.

(14) Gao, S.; Yang, J.; Liu, M.; Yan, H.; Li, W.; Zhang, J.; Luo, Y. Enhanced Photovoltaic Performance of CdS Quantum Dots Sensitized Highly Oriented Two-End-Opened TiO_2 Nanotubes Array Membrane. *J. Power Sources* **2014**, *250*, 174−180.

(15) Zheng, Z.; Xie, W.; Lim, Z. S.; You, L.; Wang, J. CdS Sensitized 3D Hierarchical TiO_2/ZnO Heterostructure for Efficient Solar Energy Conversion. *Sci. Rep.* **2013**, *4:5721*, 1−6.

(16) Lee, J. W.; Son, D. Y.; Ahn, T. K.; Shin, H. W.; Kim, I. Y.; Hwang, S. J.; Ko, M. J.; Sul, S.; Han, H.; Park, N. G. Quantum-Dot-Sensitized Solar Cell with Unprecedentedly High Photocurrent. *Sci. Rep.* **2013**, *3:1050*, 1−8.

(17) Christians, J. A.; Prashant, V.; Kamat, P. V. Trap and Transfer. Two-Step Hole Injection Across the Sb_2S_3/CuSCN Interface in Solid-State Solar Cells. *ACS Nano* **2013**, *7*, 7967−7974.

(18) Tian, J.; Uchaker, E.; Zhang, Q.; Cao, G. Hierarchically Structured ZnO Nanorods—Nanosheets for Improved Quantum-Dot-Sensitized Solar Cells. *ACS Appl. Mater. Interfaces* **2014**, *6*, 4466−4472.

(19) Yuan, H.; Lu, J.; Xu, X.; Huang, D.; Chen, W.; Shen, Y.; Wang, M. Electrochemically Deposited CoS Films as Counter Electrodes for

Efficient Quantum Dot-Sensitized Solar Cells. *J. Electrochem. Soc.* **2013**, *160*, H624−H629.
(20) Itzhakov, S.; Shen, H.; Buhbut, S.; Lin, H.; Oron, D. Type-II Quantum-Dot-Sensitized Solar Cell Spanning the Visible and Near-Infrared Spectrum. *J. Phys. Chem. C* **2013**, *117*, 22203−22210.
(21) Li, T.; Lee, Y.; Teng, H. High-Performance Quantum Dot-Sensitized Solar Cells Based on Sensitization with $CuInS_2$ Quantum Dots/CdS Heterostructure. *Energy Environ. Sci.* **2012**, *5*, 5315−5324.
(22) Shen, C.; Sun, L.; Koh, Z. Y.; Wang, Q. Cuprous Sulfide Counter Electrodes Prepared by Ion Exchange for High-Efficiency Quantum Dot-Sensitized Solar Cells. *J. Mater. Chem. A* **2014**, *2*, 2807−2813.
(23) Tian, J.; Zhang, Q.; Uchaker, E.; Gao, R.; Qu, X.; Zhang, S.; Cao, G. Architectured ZnO Photoelectrode for High Efficiency Quantum Dot Sensitized Solar Cells. *Energy Environ. Sci.* **2013**, *6*, 3542−3547.
(24) Zhao, K.; Yu, H.; Zhang, H.; Zhong, X. Electroplating Cuprous Sulfide Counter Electrode for High-Efficiency Long-Term Stability Quantum Dot Sensitized Solar Cells. *J. Phys. Chem. C* **2014**, *118*, 5683−5690.
(25) Zhou, R.; Zhang, Q.; Uchaker, E.; Lan, J.; Yin, M.; Cao, G. Mesoporous TiO_2 Beads for High Efficiency CdS/CdSe Quantum Dot Co-Sensitized Solar Cells. *J. Mater. Chem. A* **2014**, *2*, 2517−2525.
(26) McDaniel, H.; Fuke, N.; Pietryga, J. M.; Klimov, V. I. Engineered $CuInSe_xS_{2-x}$ Quantum Dots for Sensitized Solar Cells. *J. Phys. Chem. Lett.* **2013**, *4*, 355−361.
(27) Hunter McDaniel, H.; Fuke, N.; Makarov, N. S.; Jeffrey, M.; Pietryga, J. M.; Klimov, V. I. An Integrated Approach to Realizing High-Performance Liquid-Junction Quantum Dot Sensitized Solar Cells. *Nat. Commun.* **2013**, *4:2887*, 1−10.
(28) Pan, Z.; Mora-Sero, I.; Shen, Q.; Zhang, H.; Li, Y.; Zhao, K.; Wang, J.; Zhong, X.; Bisquert, J. High-Efficiency "Green" Quantum Dot Solar Cells. *J. Am. Chem. Soc.* **2014**, *136*, 9203−9210.
(29) Chakrapani, V.; Baker, D.; Kamat, P. V. Understanding the Role of the Sulfide Redox Couple (S_{2-}/Sn_{2-}) in Quantum Dot-Sensitized Solar Cells. *J. Am. Chem. Soc.* **2011**, *133*, 9607−9615.
(30) Lee, Y.-L.; Lo, Y.-S. Highly Efficient Quantum-Dot-Sensitized Solar Cell Based on Co-Sensitization of CdS/CdSe. *Adv. Funct. Mater.* **2009**, *19*, 604−609.
(31) Tachibana, Y.; Akiyama, H. Y.; Ohtsuka, Y.; Torimoto, T.; Kuwabata, S. CdS Quantum Dots Sensitized TiO_2 Sandwich Type Photoelectrochemical Solar Cells. *Chem. Lett.* **2007**, *36*, 88−89.
(32) Hodes, G.; Manassen, J. Electrocatalytic Electrodes for the Polysulfide Redox System. *J. Electrochem. Soc.* **1980**, *127*, 544−549.
(33) Ning, Z.; Tian, H.; Yuan, C.; Fu, Y.; Sun, L.; Agren, H. Pure Organic Redox Couple for Quantum-Dot-Sensitized Solar Cells. *Chem.—Eur. J.* **2011**, *17*, 6330−6333.
(34) Lee, H. J.; Yum, J. H.; Leventis, H. C.; Zakeeruddin, S. M.; Haque, S. A.; Chen, P.; Seok, S. I.; Grätzel, M.; Nazeeruddin, M. K. CdSe Quantum Dot-Sensitized Solar Cells Exceeding Efficiency 1% at Full-Sun Intensity. *J. Phys. Chem. C* **2008**, *112*, 11600−11608.
(35) Lee, H. J.; Wang, M.; Chen, P.; Gamelin, D. R.; Zakeeruddin, S. M.; Grätzel, M.; Nazeeruddin, M. K. Efficient CdSe Quantum Dot-Sensitized Solar Cells Prepared by an Improved Successive Ionic Layer Adsorption and Reaction Process. *Nano Lett.* **2009**, *9*, 4221−4227.
(36) Hao, F.; Dong, P.; Zhang, J.; Zhang, Y.; Loya, P. E.; Hauge, R. H.; Li, J.; Lou, J.; Lin, H. High Electrocatalytic Activity of Vertically Aligned Single-Walled Carbon Nanotubes towards Sulfide Redox Shuttles. *Sci. Rep.* **2012**, *368*, 1−6.
(37) Anderson, A. Y.; Barnes, P. R. F.; Durrant, J. R.; O'Regan, B. C. Quantifying Regeneration in Dye-Sensitized Solar Cells. *J. Phys. Chem. C* **2011**, *115*, 2439−2447.
(38) Barea, E. M.; Ortiz, J.; Payá, F. J.; Fernández-Lázaro, F.; Fabregat-Santiago, F.; Sastre-Santos, A.; Bisquert, J. Energetic Factors Governing Injection, Regeneration and Recombination in Dye Solar Cells with Phthalocyanine Sensitizers. *Energy Environ. Sci.* **2010**, *3*, 1985−1994.
(39) Daeneke, T.; Mozer, A. J.; Kwon, T.-H.; Duffy, N. W.; Holmes, A. B.; Bach, U.; Spiccia, L. Dye Regeneration and Charge Recombination in Dye-Sensitized Solar Cells with Ferrocene Derivatives as Redox Mediators. *Energy Environ. Sci.* **2012**, *5*, 7090−7099.
(40) Daeneke, T.; Mozer, A. J.; Uemura, Y.; Makuta, S.; Fekete, M.; Tachibana, Y.; Koumura, N.; Bach, U.; Spiccia, L. Dye Regeneration Kinetics in Dye-Sensitized Solar Cells. *J. Am. Chem. Soc.* **2012**, *134*, 16925−16928.
(41) Heimer, T. A.; Heilweil, E. J. Electron Injection, Recombination, and Halide Oxidation Dynamics at Dye-Sensitized Metal Oxide Interfaces. *J. Phys. Chem. A* **2000**, *104*, 4256−4262.
(42) Montanari, I.; Nelson, J.; Durrant, J. R. Iodide Electron Transfer Kinetics in Dye-Sensitized Nanocrystalline TiO_2 Films. *J. Phys. Chem. B* **2002**, *106*, 12203−12210.
(43) Nasr, C.; Hotchandani, S. Role of Iodide in Photoelectrochemical Solar Cells. Electron Transfer between Iodide Ions and Ruthenium Polypyridyl. *J. Phys. Chem. B* **1998**, *102*, 4944−4951.
(44) Li, F.; Jennings, J. R.; Wang, Q. Determination of Sensitizer Regeneration Efficiency in Dye-Sensitized Solar Cells. *ACS Nano* **2013**, *7*, 8233−8242.
(45) Pelet, S.; Moser, J. E.; Grätzel, M. Cooperative Effect of Adsorbed Cations and Iodide on the Interception of Back Electron Transfer in the Dye Sensitization of Nanocrystalline TiO_2. *J. Phys. Chem. B* **2000**, *104*, 1791−1795.
(46) Park, H. S.; Leonard, K. C.; Bard, A. J. Surface Interrogation Scanning Electrochemical Microscopy (SI-SECM) of Photoelectrochemistry at a W/Mo-$BiVO_4$ Semiconductor Electrode: Quantification of Hydroxyl Radicals during Water Oxidation. *J. Phys. Chem. C* **2013**, *117*, 12093−12102.
(47) Ritzert, N. L.; Rodriguez-Lopez, J.; Tan, C.; Abruna, H. D. Kinetics of Interfacial Electron Transfer at Single-Layer Graphene Electrodes in Aqueous and Nonaqueous Solutions. *Langmuir* **2013**, *29*, 1683−1694.
(48) Shen, Y.; Nonomura, K.; Schlettwein, D.; Zhao, C.; Wittstock, G. Photoelectrochemical Kinetics of Eosin Y-Sensitized Zinc Oxide Films Investigated by Scanning Electrochemical Microscopy. *Chem.—Eur. J.* **2006**, *12*, 5832−5839.
(49) Mengesha Tefashe, U.; Nonomura, K.; Vlachopoulos, N.; Hagfeldt, A.; Wittstock, G. Effect of Cation on Dye Regeneration Kinetics of N719-Sensitized TiO_2 Films in Acetonitrile-Based and Ionic-Liquid-Based Electrolytes Investigated by Scanning Electrochemical Microscopy. *J. Phys. Chem. C* **2012**, *116*, 4316−4323.
(50) Shen, Y.; Tefashe, U. M.; Nonomura, K.; Loewenstein, T.; Schlettwein, D.; Wittstock, G. Photoelectrochemical Kinetics of Eosin Y-Sensitized Zinc Oxide Films Investigated by Scanning Electrochemical Microscopy under Illumination with Different LED. *Electrochim. Acta* **2009**, *55*, 458−464.
(51) Wang, M. K.; Chamberland, N.; Breau, L.; Moser, J. E.; Baker, R. H.; Marsan, B.; Zakeeruddin, S. M.; Grätzel, M. An Organic Redox Electrolyte to Rival Triiodide-Iodide in Dye-Sensitized Solar Cells. *Nat. Chem.* **2010**, *2*, 385−389.
(52) Liu, B.; Bard, A. J.; Mirkin, M. V.; Creager, S. E. Electron Transfer at Self-Assembled Monolayers Measured by Scanning Electrochemical Microscopy. *J. Am. Chem. Soc.* **2004**, *126*, 1485−1492.
(53) Tefashe, U. M.; Rudolph, M.; Miura, H.; Schlettwein, D.; Wittstock, G. Photovoltaic Characteristics and Dye Regeneration Kinetics in D149-sensitized ZnO with Varied Dye Loading and Film Thickness. *Phys. Chem. Chem. Phys.* **2012**, *14*, 7533−7542.
(54) Boschloo, G.; Hagfeldt, A. Characteristics of the Iodide-Triiodide Redox Mediator in Dye-Sensitized Solar Cells. *Acc. Chem. Res.* **2009**, *42*, 1819−1826.